

# Latitude behavior and interrelations among the aerosol properties in the atmosphere over South Atlantic

S.M. Sakerin, D.M. Kabanov, M.V. Panchenko, and V.V. Pol'kin

*Institute of Atmospheric Optics,  
Siberian Branch of the Russian Academy of Sciences, Tomsk*

Received February 21, 2006

We present some results on the aerosol optical depth (AOD) in the wavelength region from 0.34 to 4  $\mu\text{m}$ , aerosol number concentration, and mass content of soot in the near-water atmospheric layer studied during nineteenth mission of *Akademik Sergey Vavilov* R/V (Atlantic Ocean, October–December 2004). Statistical characteristics of aerosol from separate regions of the Atlantic Ocean (tropical zone, coastal region of Cape Town, Southern Ocean, etc.) are discussed. Very low aerosol and soot content has been observed in the regions southward of 35°S; average aerosol characteristics are found to be 0.05 for AOD in the visible range (0.55  $\mu\text{m}$ ), 0.04 for AOD in IR (1.2–4  $\mu\text{m}$ ), 5.1  $\text{cm}^{-3}$  for number concentration of the near-water aerosol ( $r = 0.2\text{--}5 \mu\text{m}$ ), and 0.04  $\mu\text{g}/\text{m}^3$  for the mass concentration of soot. It is shown that it is characteristic of the atmosphere of Southern Hemisphere the observed latitudinal dependence of AOD and soot content (decrease with the growing latitude). We consider interrelations among aerosol characteristics of the near-water layer and of the entire atmospheric column.

## Introduction

Study of mechanisms and tendencies in climate change is impossible with no data available on the global variation of the climatically significant properties, among which the atmospheric aerosol plays an important part. To obtain these data, international and national systems of regular aerosol observations have been developed recently in different regions of the globe.<sup>1,2</sup> At the same time, thus obtained information mostly characterizes the continental regions. However, the atmosphere over oceans covers about 2.5 times more vast area, which has substantial differences in aerosol composition and its variability. However, the aerosol measurements are only being conducted at coastal stations (overburdened to a certain extent by the “continental influence”) and, episodically, from onboard a ship. In this regard, importance of new cycles of atmospheric aerosol study in marine campaigns becomes obvious. Analysis of the overviews of aerosol studies shows that the measurements of, e.g., atmospheric aerosol optical depth (AOD)<sup>3,4</sup> were most frequent in North and Central Atlantic (including internal seas), and much more rare in the Pacific and Indian Oceans. The atmosphere of southern part of Atlantic Ocean is quite poorly studied oceanic region.

In this paper we discuss measurements of atmospheric aerosol characteristics over Atlantic Ocean in the period of nineteenth mission of *Akademik Sergey Vavilov* R/V (October–December 2004). We consider the statistical characteristics of AOD in the wavelength range (0.34–4  $\mu\text{m}$ ) and concentration of aerosol and soot in the near-water atmospheric layer in separate regions of the Atlantic

Ocean. The main attention is paid to analysis of latitudinal behavior of aerosol characteristics and interrelations among them in the atmosphere of the Southern Hemisphere.

## 1. Experiments

During the mission, two types of aerosol experiments have been carried out: we measured atmospheric AOD using sun photometers, and measured aerosol concentration in the near-water layer using photoelectric counter and soot meter. At the time of observations, all the instruments were located on the deck of ship, where the best conditions for sky viewing and minimum influence of local aerosol sources were ensured.

SP-5 multiwavelength photometer used has three measurement channels: 1) shortwave (0.4–1.1- $\mu\text{m}$ ) channel on the basis of silicon photodiode FDUK-31; 2) infrared (1.1–4- $\mu\text{m}$ ) channel that uses an MG-32 pyroelectric detector; 3) ultraviolet (0.3–0.4- $\mu\text{m}$ ) channel with a solar-blind SiC photodiode as a detector. Separation of individual spectral intervals in the photometer is performed using interference filters mounted in continuously rotating reel. Also, photometer includes two-coordinate rotating device driven by automated sun tracking scheme. The main characteristics of the photometer are presented in Table 1.

Observations of spectral transmission were performed continuously in the periods of clear sky, when the solar zenith distance did not exceed 80°. Photometer was calibrated by the Langley method for data obtained during mission under conditions of high atmospheric transmission. Methods of calibration and calculation of AOD  $\tau_\lambda$  used are described in

Refs. 5 and 6. Error of AOD determination is 0.01–0.02 in shortwave spectral range, increasing to 0.02–0.03 in the IR channel.

**Table 1. Main characteristics of an SP-5 photometer**

Characteristics	UV channel	SW channel	IR channel
Field of view, deg	0.92	1.5	1.15
Maxima of filters, $\mu\text{m}$	0.34; 0.37	0.42; 0.44; 0.48; 0.55; 0.63; 0.68; 0.78; 0.87; 0.94; 1.06	1.24; 1.56; 2.15; 4
Bandwidth of the filter (FWHM), nm	5–8	5–15	10–50
Duration of single cycle, s		50	

In analysis, we used 30-min average values of  $\tau_\lambda$  and Angström exponent  $\alpha$ ,<sup>7</sup> which characterizes selectivity of the spectral dependence of AOD in shortwave spectral range:

$$\tau(\lambda) = \beta\lambda^{-\alpha}.$$

Parameters  $\alpha$  and  $\beta$  were calculated by the least squares method after taking logarithm of this dependence in the wavelength region 0.34–0.87  $\mu\text{m}$ .

For determination of aerosol characteristics in the near-water atmospheric layer, we used the instrumentation developed and manufactured at the IAO SB RAS. The aerosol number concentration was measured with an upgraded photoelectric particle counter based on a commercial AZ-5 device. Its main specifications are as follows: size range of measurable particles is 0.2 to 5  $\mu\text{m}$ ; number of channels (subintervals of particle sizes) is 256; air flow pump-through rate is 1.2 l/min; duration of a measurement cycle in the standard sampling mode is 10 to 15 min.

The soot (black carbon (BC)) mass content was measured using a soot meter,<sup>8</sup> whose principle of operation is analogous to that of devices of the type of aethalometer.<sup>9</sup> The aethalometer operation is based on the measurement of light extinction due to diffuse scattering by the layer of aerosol particles sampled onto a filter from the air flow pumped through. In this case, the extinction of light by the layer of particles recorded is directly proportional to surface concentration of aerosol substance on the filter and, hence, to its mass concentration in air.<sup>10,11</sup> The calibration was made by comparing with data of the optical and gravimetric measurements of the soot aerosol properties.

The sampling device common for the photoelectric particle counter and aethalometer was mounted in the laboratory; and sampling tubes went out of the ship interior oriented onward the direction of ship motion at the height about 2 m above the deck and about 16 m above the water surface. The

measurements were performed every half an hour or hourly during a day and sometimes at night.

The ship route (Fig. 1) started in Kaliningrad and then through the English Channel to Cape Town. The measurements have been conducted along the route at the sites in Atlantic sector of Southern Ocean. Measurements of the aerosol characteristics in the near-water layer began yet in Baltic Sea, and those of atmospheric transmission after entering the Atlantic Ocean. All the measurements ended on December 5–6, 2004 in the region of Ushuaya (Terra del Fuego island, Argentina).

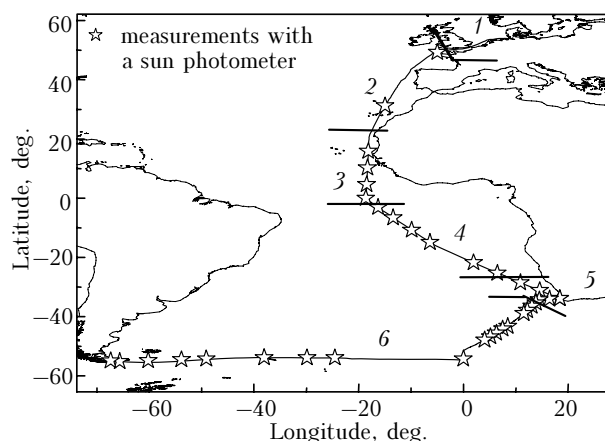


**Fig. 1.** Map of the aerosol studies region: Baltic and North Seas (curve 1); midlatitudes of Atlantic (the route leg from Bay of Biscay to Canary islands) (curve 2); northern trade-wind zone (curve 3); tropical South Atlantic (curve 4); “Cape Town” (curve 5); Southern Ocean (curve 6).

Tables 2 and 3 give information on the bulk of the data obtained and on meteorological conditions.

**Table 2. Volume of the obtained data**

Instrument	Measurement period	Number of measurement days	Number of cycles
SP-5 Sun photometer	10/23–12/05	34	1768
“Aerosol complex”	10/12–12/05	61	1205

**Table 3. Meteorological characteristics in different regions: means (min–max)**

Region (Fig. 1)	Temperature, °C	Relative humidity, %	Absolute humidity, g/m <sup>3</sup>	Wind speed, m/s
2	19.3 (13–25)	92 (56–97)	21.3 (12–30)	7.7 (1–15)
3	26.1 (22–31)	81 (67–97)	27.4 (22–32)	6.9 (1–10)
4	21.4 (18–27)	74 (70–81)	18.9 (15–25)	5.9 (1–13)
5*	19.4 (16–24)	68 (38–88)	15.2 (11–19)	6.9 (0–17)
6	7.4 (–1–22)	82 (48–97)	9.2 (4–19)	8.3 (1–21)

\* Gap in meteorological measurements between November 5 and 9 was filled with data of actual weather conditions in the region of Cape Town [http://www.gismeteo.ru].

## 2. Statistics and interrelations of the aerosol characteristics

### Atmospheric AOD

The atmospheric AOD varies quite widely (Fig. 2) because the aerosol turbidity has specific regional features associated with aerosol outflow off the continent.<sup>3,4,6</sup>

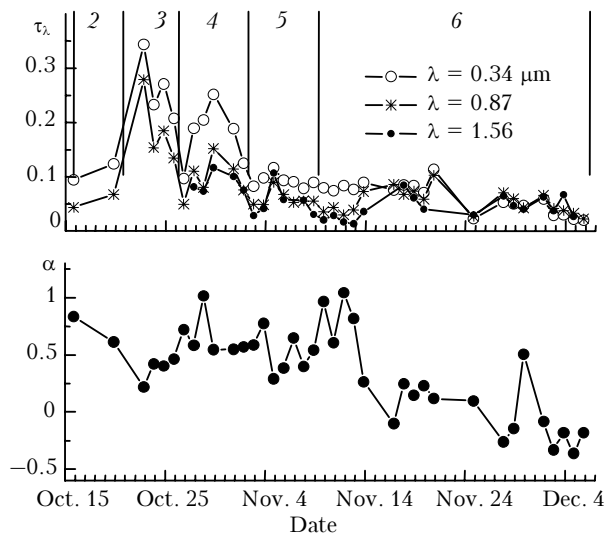


Fig. 2. Variations of daily mean  $\tau_\lambda$  and  $\alpha$  during the mission.

In view of the presence of spatial inhomogeneities, it is reasonable to consider the statistics of AOD variations within separate regions. In South Atlantic, we identified three regions: “tropical zone,” with six days of measurements in the period from October 27 to November 2; coastal region of Cape Town, with seven measurement days in the period from November 3 to November 9; and Southern Ocean from 34° to 55°S, with nineteen days in the period from November 10 to December 6. The statistical characteristics of  $\tau_\lambda$  for the entire spectral region were already reported earlier<sup>12</sup>; therefore, here we will only consider average data (Fig. 3) and compare them with results of other authors (Table 4).

In contrast to “north trade-wind”,<sup>3,6</sup> in the south tropical zone the atmospheric turbidity is not high. At the same time, this region is characterized by the largest AOD and Angström exponent, when

compared with other regions of the Southern Hemisphere. Possible causes for elevated AOD values in the mid-Atlantic region may be: weakened influence of loess dust blown by Harmatan wind<sup>3</sup> and/or influence of continental aerosol from Saint Helena Island (maximum  $\tau_\lambda$  values were observed during passage near the island). Quite close values were obtained in other studies in this region (see Table 4).

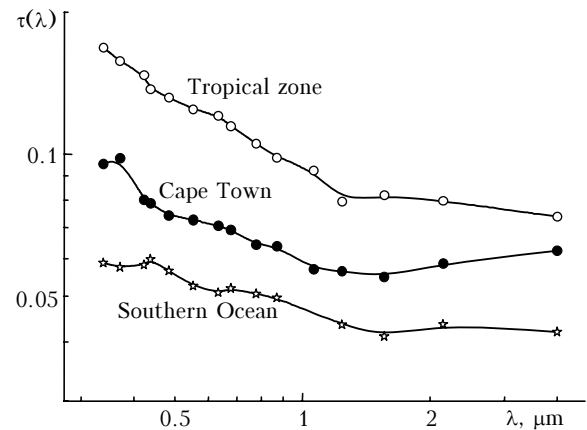


Fig. 3. Average spectral dependences  $\tau(\lambda)$  in three regions of South Atlantic.

Unexpectedly low AOD values were found in the coastal region of Cape Town. From the comparison with the data from Ref. 14 it is seen that the average  $\tau_\lambda$  and  $\alpha$  in the region of Cape Town are 2 to 3 times higher than in the coastal regions of the Northern Hemisphere; however, they well agree with data in central-oceanic region of the Pacific Ocean. The high atmospheric transmission in the region of Cape Town seems to be caused by two reasons: 1) predominating wind from ocean in the period of observations; and 2) lower continental (including anthropogenic) aerosol content than in analogous regions of Northern Hemisphere.

Minimum aerosol turbidity was observed over Southern Ocean; the values of  $\tau_\lambda$  here were found to be lower than in the regions of the Pacific Ocean,<sup>14</sup> no less removed from the land. In addition, we noticed relative stability of AOD: aerosol turbidity did not increase even during approach to Ushuaya (South America). The low values of  $\alpha$  and  $\tau_\lambda$  in the entire spectral range are an evidence of the low content of both fine and coarse aerosol.

Table 4. Comparative data for main atmospheric AOD characteristics

Region	$\tau_{0.55} \pm \sigma_\tau$	$\alpha \pm \sigma_\alpha$	$\tau_c$	$\tau_f$	Data of other authors
Tropical zone	$0.125 \pm 0.038$	$0.52 \pm 0.11$	0.087	0.038	Ascension Island <sup>3</sup> : $\tau_{0.5} = 0.13$ , $\alpha = 0.2$ Forty third mission of Prof. Vize R/V <sup>4</sup> : $\tau_{0.5} = 0.09$ , $\alpha = 0.3$ Our data for 1989 and 1995 <sup>13</sup> : $\tau_{0.55} = 0.14$ , $\alpha = 0.85$
“Cape Town”	$0.073 \pm 0.03$	$0.43 \pm 0.26$	0.060	0.013	Coastal regions <sup>14</sup> : $\tau_{0.55} = 0.2$ , $\alpha = 0.9$
Southern Ocean	$0.053 \pm 0.018$	$0.20 \pm 0.35$	0.042	0.011	Central Pacific Ocean <sup>14</sup> : $\tau_{0.55} = 0.07$ , $\alpha = 0.4$ Antarctic (Mirny station) <sup>4</sup> : $\tau_{0.55} = 0.05$

Of independent interest is the question on the magnitude and spectral dependence  $\tau(\lambda)$  at the wavelengths longer than  $1 \mu\text{m}$ . The results of not numerous studies in the IR atmospheric transmission windows<sup>6,15–17</sup> indicate that  $\tau(\lambda)$  may have both neutral behavior and deviate from it. The studies carried out in the nineteenth mission have shown that the differences in AOD at some wavelengths from the spectral region  $1.2\text{--}4 \mu\text{m}$  are insignificant and do not exceed 0.03.

The data available on  $\tau(\lambda)$  in the long-wave spectral region make it possible to estimate the contribution of fine and coarse aerosol to AOD. Remind that the optical influence of small droplets ( $r < \lambda$ ) is manifested in the form of power-law decay of aerosol extinction with increasing wavelength. The fine aerosol fraction has a significant effect from UV spectral region and up to  $1\text{--}1.5 \mu\text{m}$ . The efficiency of extinction by large particles practically does not change with wavelength and is usually assumed constant in the spectral region  $\lambda < r$  (from UV spectral range to  $2\text{--}4 \mu\text{m}$ , in our case). This property is widely used in separating optical contributions of the two aerosol fractions. Note also that redistribution of the content of small and large particles in aerosol disperse composition is one of the reasons of variations in the selectivity of spectral behavior of  $\tau(\lambda)$  and Angström exponent.

We took the average AOD values in wavelength range  $1.2\text{--}4 \mu\text{m}$  as the  $\tau_c$  component caused by the coarse aerosol fraction. The component  $\tau_f$  caused by the fine aerosol fraction varies with wavelength; therefore, we will consider it for the middle of the visible wavelength range as “residual” aerosol depth in the region  $0.55 \mu\text{m}$ :  $\tau_f = (\tau_{0.55} - \tau_c)$ . The average  $\tau_c$  and  $\tau_f$  values in three regions of South Atlantic are given in the fourth and fifth columns of Table 4.

From the data obtained, it follows that the optical effect of small particles is very weak. Their relative contribution to AOD is 2–4 times lower than  $\tau_c$ . In absolute value  $\tau_f$  gradually decreases and in the region of Southern Ocean its contribution is comparable with the measurement error.

### Near-water aerosol content

Because the measurement technique is an *in situ* one, the characteristics of aerosol concentration in near-water layer are stronger subject to the effect of local factors (rather than long-range transport) and experience much stronger variations than AOD. Among the main factors of additional fluctuations are: the spatial inhomogeneities of aerosol fields; the effects of ship-generated and other nearby aerosol sources, as well as the influence of short-scale (e.g., diurnal) variations of hydrometeorological conditions. Therefore, in analysis of results, we performed sorting out of the part of data (outliers), as being clearly local. The spatiotemporal variations of near-water aerosol were estimated for the following

characteristics: BC mass concentration  $M_s$ ; total number concentration  $N_\Sigma$  of particles with radii from  $0.2$  to  $5 \mu\text{m}$ ; concentration of fine aerosol fraction  $N_1$  ( $r = 0.2\text{--}0.5 \mu\text{m}$ ) and larger particles  $N_2$  ( $r = 0.5\text{--}1 \mu\text{m}$ ); integral parameter  $N_1/N_2$  characterizing the ratio of particle concentrations in two size ranges.

The specific features of variations of the  $N_\Sigma$ ,  $N_1/N_2$ , and  $M_s$  values are illustrated in Fig. 4.

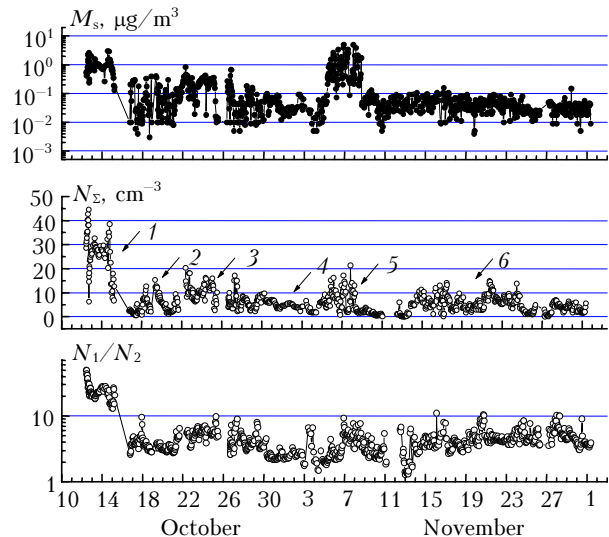


Fig. 4. Variations of the main characteristics of near-water aerosol.

The variability ranges of aerosol characteristics for the period under study (min–max) were: total concentration  $N_\Sigma = 0.01\text{--}45 \text{ cm}^{-3}$ ; ratio of the fractions  $N_1/N_2 = 1.3\text{--}50$ ; and absorber mass content  $M_s = 10^{-3}\text{--}5 \mu\text{g}/\text{m}^3$ . For analysis of time variations, we calculated the statistical characteristics for six regions (see Fig. 1). Clear demonstration of the specific features of aerosol disperse composition in these regions follows from analysis of differential distribution of particle concentration  $n_i$  (Fig. 5).

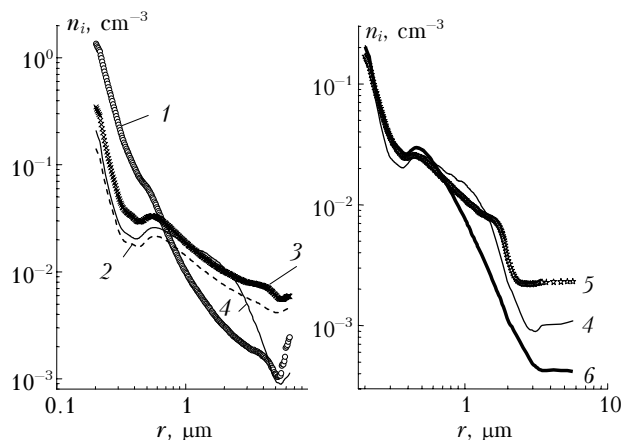


Fig. 5. Differential aerosol concentrations in different regions of Atlantic.

Based on statistical characteristics (Table 5), we can identify three regions (1, 3, and 5), where the

effect of continental aerosol is most significant. Aerosol has maximum content and strongest variations in Baltic and North Seas, i.e., in the regions of transport of air masses from industrially developed European countries. Elevated aerosol content in these regions is 3–6 times higher than elsewhere, primarily due to the presence of small-sized particles (see Fig. 5). Quantitatively, this is obviously seen from the fact that for two fractions the ratio of concentrations  $N_1/N_2$  exceeds 24, whereas in all other regions it slightly varies between 3.5 and 5.5. The atmosphere of Baltic and North Seas is also distinctly characterized by the largest content of absorbers  $M_s$  in atmospheric aerosol, on average about  $1 \mu\text{g}/\text{m}^3$ .

Next region with a significant level of aerosol concentration is the zone of trade-wind-blown dust aerosol (region 3), known as Darkness Sea (see Ref. 3 and others). Interestingly, an additional enrichment with continental aerosol generally takes place over

the entire optically active particle size range; however, in the given measurement period it has been more marked in the submicron range of particle sizes. The BC content in the trade-wind zone is also elevated but not that high as in Cape Town region. The characteristic features of the coastal region (5) include large concentration of absorbing aerosol and strong relative variations of all aerosol characteristics. Obvious causes of variations are proximity to powerful sources of continental (including anthropogenic) aerosol and generation of maritime aerosol in surf zone.

Three other regions (2, 4, and 6) experience the continental effect to a lower degree and the concentration  $N_\Sigma$  there is lower. Based on average data, the most clean atmosphere is over Southern Ocean, with  $N_\Sigma \sim 5.1 \text{ cm}^{-3}$ , and  $M_s = 0.04 \mu\text{g}/\text{m}^3$ . Nonetheless, note that the differences (between regions 2, 4, and 6) in the mean values are smaller than the standard deviation  $\sigma$ .

**Table 5. Statistics of the main characteristics of near-water aerosol**

Region	Aerosol concentration $N_\Sigma$ , $\text{cm}^{-3}$				Mean value			BC mass content $M_s$ , $\mu\text{g}/\text{m}^3$			
	Mean value	$\sigma$	min	max	$N_1/N_2$	$N_1$	$N_2$	Mean value	$\sigma$	min	max
1	26.4	8.35	6.2	44.5	24.3	24.9	1.06	0.959	0.594	0.01	3.05
2	4.63	3.47	0.56	15.3	3.68	2.86	0.82	0.082	0.101	0.003	0.405
3	8.78	4.58	2.12	20.4	5.50	6.26	1.18	0.192	0.137	0.008	0.833
4	5.57	2.46	1.72	17.0	3.47	3.57	0.98	0.056	0.072	0.001	0.674
5	5.43	3.57	0.78	16.1	3.64	3.39	1.07	0.440	0.47	0.018	1.89
6	5.08	3.23	0.05	16.9	4.58	3.04	1.53	0.040	0.022	0.005	0.148
Tomsk	10.8	—	0.385	244	72	10	0.237	1.37	—	0.058	16.4

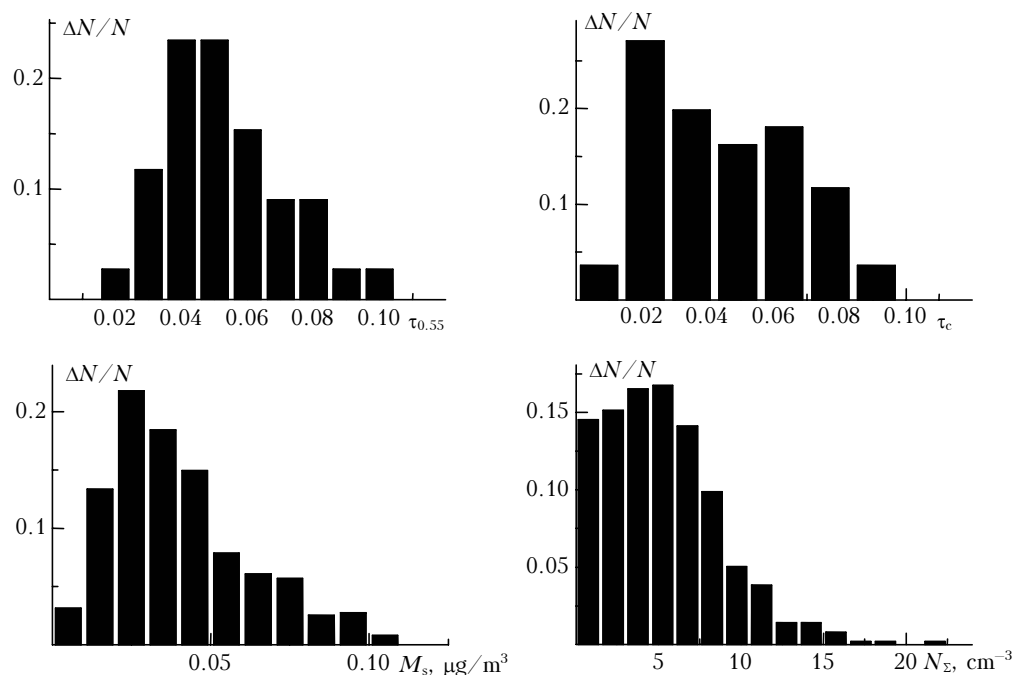


**Fig. 6. Interrelations of aerosol characteristics (Southern Hemisphere).**

The distribution of aerosol number concentration over these Atlantic regions overall agrees with the data of international and Russian experiments, such as TROPEX-72, ATEP-74, POLEX-South-81, and thirteen mission of *Priliv R/V*.<sup>3</sup> For instance, the measurement data in Southern Ocean waters (55–65°S) in 1987 indicated that the average  $N_{\Sigma}$  value was  $4.4 \text{ cm}^{-3}$  and varied from  $2.2$  to  $6.6 \text{ cm}^{-3}$  for different wind directions.

To compare typical aerosol concentrations in the continental atmosphere, the results of many-year observations near Tomsk<sup>18,19</sup> are given in the lower part of the Table 5. The comparison shows that aerosol content in near-water and near-ground atmospheric layers differs substantially. The concentration of small droplets is approximately three times higher under continental conditions, whereas atmosphere over ocean has much more larger-sized particles. As a consequence, the ratio of concentrations  $N_1/N_2$  between the two fractions differs by more than an order of magnitude for the two regions. No less significant is the difference in BC mass concentration. In the pure oceanic regions (2, 4, and 6), the soot content is approximately (on the average) 20 times lower; however, this difference rapidly decreases while approaching the zones of continental outflows (1 and 5).

In conclusion of this section, we shall consider the frequency distributions of aerosol characteristics. In order to exclude dealing with the effects of spatial inhomogeneities, we shall consider the region of Southern Ocean, where most of the data have been collected. The calculated histograms of distributions of the main characteristics are shown in Fig. 6, from which it is seen that the distributions of  $\tau_{0.55}$ ,  $M_s$ , and  $N_{\Sigma}$  are unimodal and skewed toward larger values.

The data presented make it possible to estimate the most probable (modal) values of these characteristics, i.e.,  $(\tau)_m \sim 0.045$ ,  $(M_s)_m \sim 0.03$ , and  $(N_{\Sigma})_m \sim 5$ . The histogram of  $\tau_c$  has two modes with the main mode in the region  $\sim 0.02$  and less pronounced mode at  $\sim 0.06$ .

### Interrelations among aerosol characteristics

It is interesting to estimate the interrelations among two groups of aerosol characteristics, i.e., those of the entire atmospheric column and in the local near-water layer. Parameters of the first group will be  $\tau_{0.55}$ ,  $\tau_c$ , and  $\tau_f$ , and in the second group the parameters  $N_{\Sigma}$ ,  $N_1$ ,  $N_2$ , and  $M_s$ . These characteristics differently respond to the effect of local sources and transport of aerosol from the neighbor regions (and, in particular, from continents). The near-water atmospheric layer is in the immediate vicinity of the water surface. Therefore, the instruments measuring concentration faster respond to intensity of generation of marine aerosol (unfortunately, they are more subject to distortions by the ship). Atmospheric AOD is an integrated characteristic of aerosol

content at different altitudes; therefore, it is much stronger affected by aerosol transport from other regions. It should also be kept in mind that AOD and concentration are quite different characteristics indeed. The parameter  $\tau_{\lambda}$  (and its components  $\tau_c$  and  $\tau_f$ ) is not only the function of aerosol content in the atmosphere, but also efficiency of extinction of radiation, which depends on relative particle size.

To calculate the correlation coefficients  $R_{i,j}$ , we used an array of hourly mean aerosol characteristics obtained in the Southern Hemisphere (regions 4–6), excluding only data collected during the stay in Cape Town. The character of interrelations between some parameters is shown in Fig. 7, and the calculated coefficients  $R_{i,j}$  are presented in Table 6. For the considered data array, the critical correlation with confidence probability 0.95 is 0.253.

The high correlations of  $\tau_{0.55}$  with two its components  $\tau_f$  and  $\tau_c$  (and, analogously, correlation of  $N_{\Sigma}$  with  $N_1$  and  $N_2$ ) need no additional comments. We only indicate the higher correlation coefficient of the component  $\tau_c$ , stronger contributing to  $\tau_{0.55}$ . The absence of correlation between  $\tau_f$  and  $\tau_c$  suggests that variations of the coarse and fine aerosol fractions in the atmospheric column have different origin. At the same time, in near-water atmospheric layer, there is high correlation between aerosol concentrations in the two size ranges. Seemingly, this is because the considered size range ( $r = 0.2\text{--}0.5\text{--}1 \mu\text{m}$ ) is relatively narrow, and within it the dominating contribution to  $N_1$  and  $N_2$  variations comes from the common mechanism, namely, generation of marine aerosol.

**Table 6. Coefficients of correlation between AOD and aerosol concentration in the near-water layer (entries in bold show significant correlation)**

Parameter	$\tau_{0.55}$	$\tau_c$	$\tau_f(0.55)$	$M_s$	$N_{\Sigma}$	$N_1$	$N_2$
$\tau_{0.55}$	1	<b>0.80</b>	<b>0.70</b>	0.03	<b>0.29</b>	0.10	<b>0.45</b>
$\tau_c$		1	0.13	0.08	<b>0.48</b>	<b>0.34</b>	<b>0.60</b>
$\tau_f(0.55)$			1	-0.07	-0.12	-0.26	0.02
$M_s$				1	0.16	0.19	0.13
$N_{\Sigma}$					1	<b>0.97</b>	<b>0.95</b>
$N_1$						1	<b>0.85</b>

Among the characteristics in different groups, the strongest correlation is observed between  $\tau_c$  and  $N_2$ . Therefore,  $\tau_c$  is markedly influenced by the contribution of the local marine aerosol in the size range  $r > 0.5 \mu\text{m}$ .

Somewhat lower, but nonetheless significant correlation is observed between  $\tau_c$  and concentration  $N_1$ , which also depends on generation of marine aerosol. The fine-mode component  $\tau_f$  is not correlated with  $N_1$ . This makes it possible to conclude that they have different sources: the composition of  $N_1$  is dominated by particles formed over sea surface, whereas  $\tau_f$  is mainly affected by long-range transport and formation of secondary (photochemical) aerosol in the atmosphere.

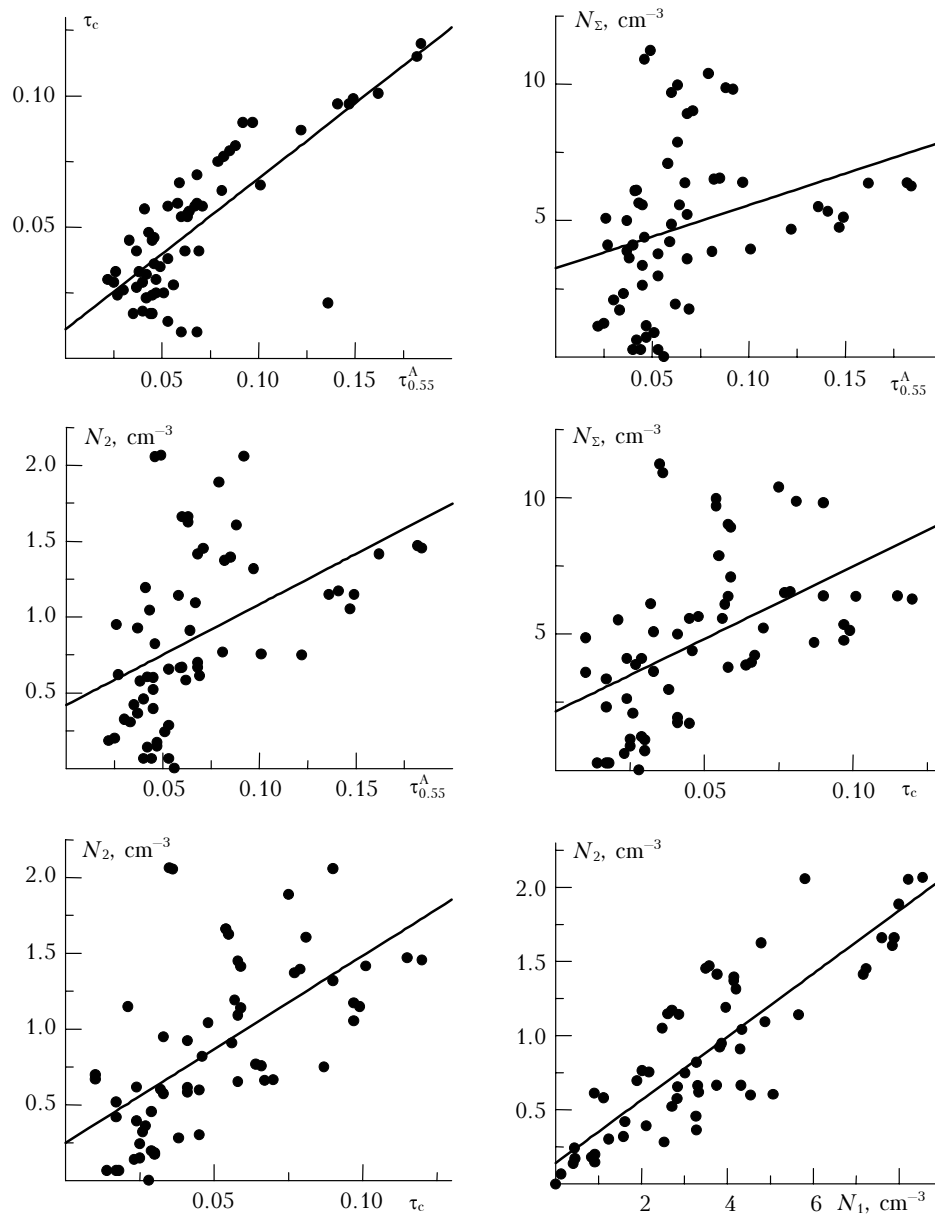


Fig. 7. Histograms of distributions of main characteristics (Southern Ocean).

At last, BC mass content correlates with none of other characteristics. This is primarily because both  $\tau_\lambda$  and number concentration just characterize aerosol content, and do not depend directly on the presence or absence of absorbing component,  $M_s$ .

### 3. Latitude dependence of aerosol characteristics in the Southern Hemisphere

#### Atmospheric AOD

As already noted above,  $\tau_\lambda$  and  $\alpha$  decrease while moving off from the equator. Furthermore, this tendency is not related with the distance from a

particular source of continental aerosol. Moreover, approaching the coastal regions (“Cape Town” and Terra del Fuego island) practically does not distort the general pattern. As an example, Figs. 8a and b show changes of  $\tau_{0.55}$  and  $\tau_c$  with latitude and two types of approximation (linear and exponential).

The latitude dependence of  $\tau_\lambda$  is evident at all wavelengths and for both AOD components. From Fig. 8 it is seen that  $\tau_{0.55}$  decreases from  $\sim 0.13$  in tropical zone to 0.048 at the latitude  $\sim 54^\circ\text{S}$ . Analogously, the coarse-mode component  $\tau_c$  decreases from  $\sim 0.09$  to 0.046. We failed to attribute this decrease to wind, influencing the generation of marine aerosol,<sup>15,20</sup> or to relative humidity. In Southern Ocean, these characteristics were on the average higher than in other regions (see Table 3).

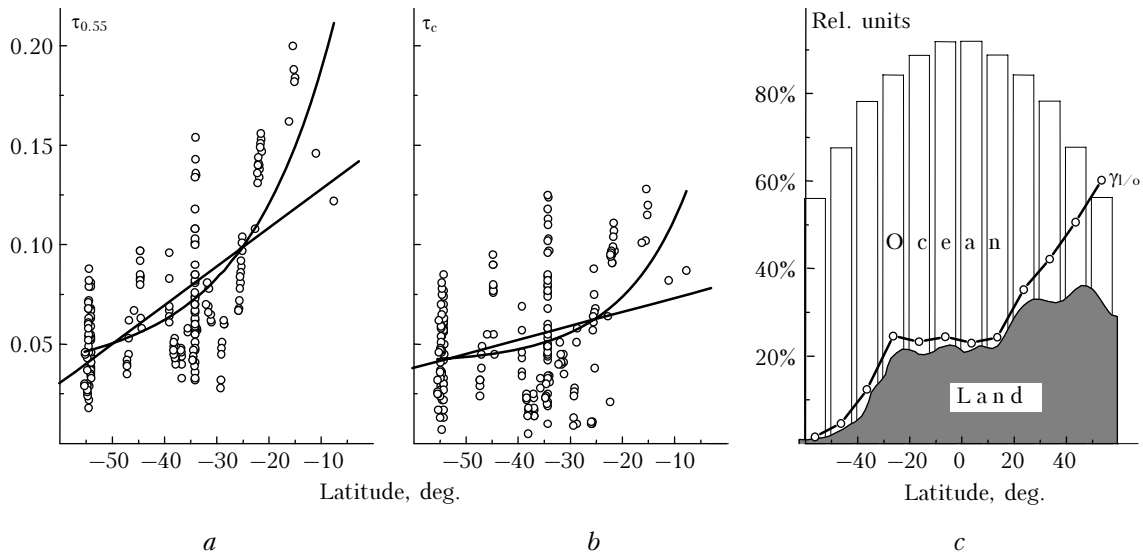


Fig. 8. Latitude variations of atmospheric AOD (*a*, *b*) and interrelations of areas occupied by land and ocean (*c*).

The latitude dependence of AOD in South Atlantic can be explained as follows. An important role in additional enrichment of the marine atmosphere with continental aerosol is played not only by proximity to continents, but also by two other factors: latitude distribution of continental aerosol sources and global circulation of air masses, in which the zonal circulations dominate. As known, the distribution of land over planet is very nonuniform, with most of its territory concentrated in the Northern Hemisphere, and with the presence of only tip of South America, New Zealand island, and ice-covered Antarctic southward of 40°S. As a quantitative confirmation, Fig. 8c shows (based on data of monograph by Neshiba<sup>21</sup>) the distribution (over latitude zones) of relative area occupied by land and ocean, as well as the ratio of these areas,  $\gamma_{\%}$ . Since significant sources of continental aerosol are absent in the middle and high latitudes of Southern Hemisphere, AOD in these regions approaches some background values, characteristic of Antarctic (see, e.g., Ref. 3).

This explanation does not contradict the fact that the central regions of the Pacific Ocean<sup>14</sup> (see Table 4) are farther removed from the continent, while the average AOD coincides with our data in the coastal region of Cape Town and exceeds that in the Southern Ocean. This is because the Pacific region<sup>14</sup> is closer to equator, in the region of zonal air circulations between the continents. Therefore, the additional contribution of continental aerosol must be larger than in high-latitude regions. Transmission study in the southern part of the Pacific, to the author's knowledge, was not performed; however, from the above considerations, the AOD in these regions also should have minimum values, close to those in the Atlantic sector of Southern Ocean and in Antarctic.

The decrease of the Angström exponent from 0.52 in the tropics to 0.2 in high latitudes of the South Atlantic is due to the influence of different latitude variations of these two aerosol fractions and

the corresponding redistribution of optical contribution to  $\tau(\lambda)$  from these fractions. From data of Table 4 it is easy to estimate that the relative value  $\tau_r/\tau_c$  is 44% in the tropical zone and decreases to 26% in the Southern Ocean. Naturally, as the relative contribution of the fine-mode component  $\tau_r$  reduces, the selectivity of AOD spectral dependence (or the value of the parameter  $\alpha$ ) decreases.

### Near-water aerosol

To detect the latitude dependence of aerosol characteristics in the near-water layer, we have excluded from the consideration the measurement data acquired during our stay in Cape Town and calculated sliding average (over 15-point window) of data, which allowed us to smooth out small-scale variations.

The obtained latitude variations of the BC mass concentration and particle concentration in different size ranges are shown in Fig. 9. The solid lines show the sliding average, and dashed line is linear fit. Certain latitude dependence of the BC content (Fig. 9a) can be seen in this figure,  $M_s$  decreases on average from 0.06  $\mu\text{g}/\text{m}^3$  at equator to  $\sim 0.03 \mu\text{g}/\text{m}^3$  at latitudes southward of 50°. At the same time, there are two regions on the general pattern, with a more rapid BC decrease up to southern latitudes  $\sim 30^\circ$ , followed by growth and continued decrease of an absorber content. We should like to note that recent studies<sup>22</sup> in Indian Ocean also revealed the latitude dependence of the BC. The BC mass content in Southern Hemisphere decreased from 0.2–0.3  $\mu\text{g}/\text{m}^3$  in equatorial zone to less than 0.05  $\mu\text{g}/\text{m}^3$  in Indian sector of the Southern Ocean (up to 56°S).

Situation with the total aerosol concentration  $N_\Sigma$  is somewhat different (Fig. 9b). The  $N_\Sigma$  variation pattern also has two regions: from equator to Cape Town (34°S) the concentration  $N_\Sigma$  does decrease with latitude (from approximately 6.5 to 3.5  $\text{cm}^{-3}$ ), but

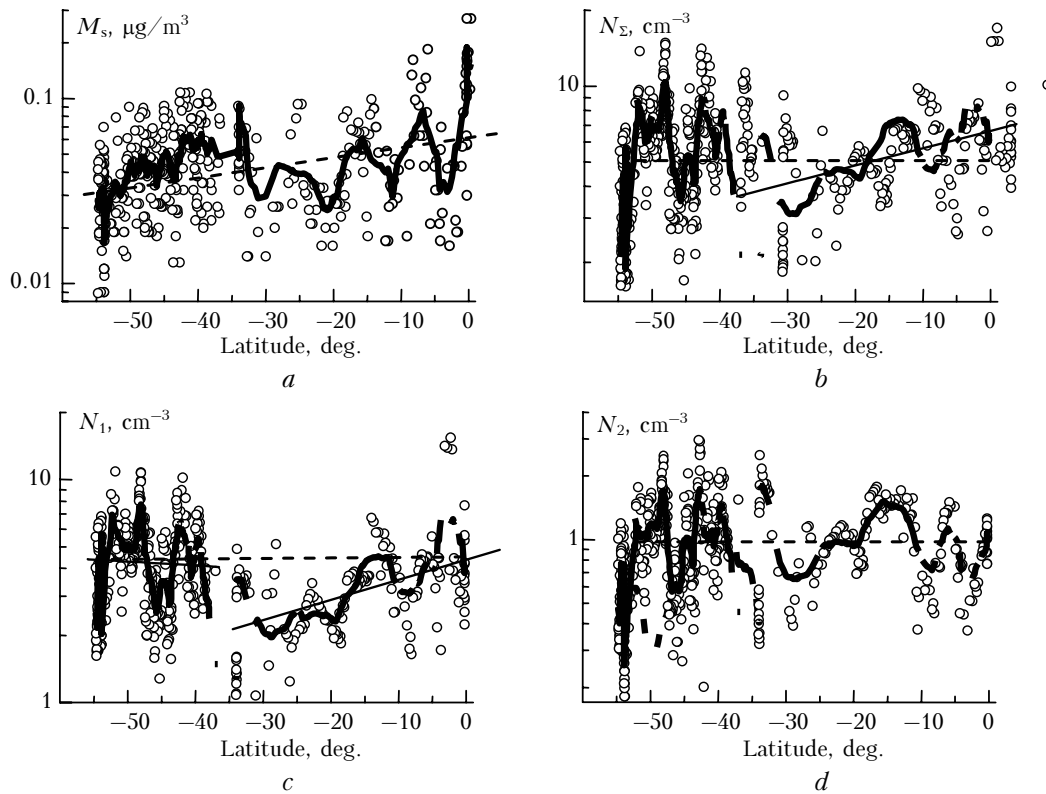


Fig. 9. Latitude variations of BC mass concentration and particle concentration,  $N_{\Sigma}$ ,  $N_1$ , and  $N_2$ .

then aerosol content recedes to higher values and after that it varies about the average level  $\sim 5 \text{ cm}^{-3}$ . Note that the latitude variations and almost jump-like growth of total ozone concentration during transit to the Southern Ocean occurred in the size range of small particles  $N_1$  (Fig. 9c). Contribution of larger particles to the total number concentration  $N_{\Sigma}$  is small and almost does not influence the view of the latitude dependence of concentration in the near-water layer.

The considered increase of concentration  $N_1$  in moving to the zone  $40\text{--}54^\circ\text{S}$  needs for further investigations. Here we only note that in that period the hydrometeorological conditions quite markedly changed (see Table 3). Possibly, combination of large wind speeds and relative humidity in Southern Ocean has led to an increase of the number of aerosol particles in the entire size range of optically active particles, in which photoelectric particle counter measurements are made. However, under conditions of high wind the concentration of large particles  $N_2$  could have been underestimated (because part of the particles may sediment in sampling device), what may explain why the growth of concentration of only small particles has been observed.

To test the statistical confidence of the decrease of aerosol characteristics with latitude, we additionally calculated the corresponding cross (aerosol characteristic – latitude) correlation coefficients. The calculations have shown that the latitudinal behaviors of  $\tau_{\lambda}$  and  $M_s$  are statistically significant

with the confidence probability 0.95 (in the case of  $N_{\Sigma}$  this is observed only in the region  $0\text{--}34^\circ\text{S}$ ). Thus, the latitude dependence was detected only for those characteristics, which are undergo relatively stronger influence by long-range aerosol transport from continent, than by local factors of generation of maritime aerosol. More specifically, these are the integrated characteristic  $\tau_{\lambda}$  and concentration of absorbing matter, more abundant in composition of continental than marine aerosol. More complicated is the dependence of number concentration of small droplets; it is caused by a combination of factors such as influence of long-range transport, decreasing with latitude (up to  $\sim 34^\circ\text{S}$ ), and effect of local factors of generation of marine aerosol (Southern Ocean waters). Finally, no effect of long-range transport is present in variations of the concentration  $N_2$ .

## Conclusion

The experiments conducted during the nineteenth mission of *Akademik Sergey Vavilov* R/V substantially increased information on the properties of atmospheric aerosol in poorly studied oceanic regions. We have determined the statistical characteristics of atmospheric AOD, aerosol mass concentration, and soot mass content in near-water layer for a few regions of Central and South Atlantic. The data analysis performed allows us to arrive at the following conclusions.

1. The atmosphere over South Atlantic (in comparison with the North Atlantic) is characterized by lower aerosol content. In the Southern Hemisphere, the most clean region is Southern Ocean, in which the mean values of main characteristics are  $\tau_{0.55} = 0.053$  ( $\alpha = 0.20$ ),  $N_{\Sigma} \sim 5.1 \text{ cm}^{-3}$ , and  $M_s = 0.04 \text{ }\mu\text{g}/\text{m}^3$ , with their most probable values being 0.045,  $5 \text{ cm}^{-3}$ , and  $0.03 \text{ }\mu\text{g}/\text{m}^3$ , respectively.

2. The AOD value in the entire spectral interval, on the average, decreases with the growth of latitude; e.g.,  $\tau_{0.55}$  decreases from  $\sim 0.13$  in the tropical zone to 0.048 southward of  $50^\circ\text{S}$  (in the IR spectral range,  $\tau_c$  decreases from  $\sim 0.08$  to 0.046). Analogous dependence has also been revealed for BC mass concentration; average  $M_s$  values decrease from  $0.06 \text{ }\mu\text{g}/\text{m}^3$  at the equator to  $\sim 0.03 \text{ }\mu\text{g}/\text{m}^3$  in the Southern Ocean. We have proposed an explanation that the observed latitude dependence is caused by weaker influence of long-range transport of the continental aerosol because of zonal character of air transport and due to a decrease of the area of land with the growth of latitude.

3. The spectral dependence  $\tau(\lambda)$  in the IR range is practically neutral, and the maximum "inter-wavelength" deviations do not exceed 0.03. The average AOD values in the wavelength range 1.2–4  $\mu\text{m}$  are 0.09 in the tropical zone, 0.06 in the region of Cape Town, and 0.04 in the Southern Ocean.

4. Analysis of interrelations among the aerosol characteristics (in the near-water layer and in the entire atmospheric column) has shown that the correlations are maximum between  $\tau_\lambda$  and two its components  $\tau_f$  and  $\tau_c$ , and, analogously, between  $N_\Sigma$  and components  $N_1$  and  $N_2$ . For the characteristics from different groups, the correlation is maximum between  $\tau_c$  and  $N_2$  and  $N_\Sigma$ . This indicates that the AOD component caused by the coarse aerosol is dominated by local marine aerosol with the size  $r > 0.5 \text{ }\mu\text{m}$ .

### Acknowledgments

Authors thank V.S. Kozlov and V.P. Shmargunov for technical preparation of instrumentation and kindly provided instruments for study the soot constituent of the aerosol.

This study has been supported by the Program of Basic Research of the Presidium of RAS "Basic problems in oceanology: physics, geology, biology, and ecology."

### References

1. WMO/GAW Expert's Workshop on a Global Surface-Based Network for Long Term Observations of Column Aerosol Optical Properties. Report No. 162 (WMO TD No. 1287) (Davos, Switzerland, 2005), 144 pp.
2. B.N. Holben, T.F. Eck, I. Slutsker, D. Tanre, J.P. Buis, A. Setzer, E. Vermote, J.A. Reagan, Y.J. Kaufman, T. Nakadjima, F. Lavenu, I. Jankowiak, and A. Smirnov, *Remote Sens. Environ.* **66**, 1–16 (1998).
3. A. Smirnov, B.N. Holben, Y.J. Kaufman, O. Dubovik, T.F. Eck, I. Slutsker, C. Pietras, and R.N. Halthore, *J. Atmos. Sci.* **59**, No. 3, Part 1, 501–523 (2002).
4. O.D. Barteneva, N.I. Nikitinskaya, G.G. Sakunov, and L.K. Veselova, *Transmission of Atmospheric Depth in Visible and IR Spectral Region* (Gidrometeoizdat, Leningrad, 1991), 224 pp.
5. D.M. Kabanov and S.M. Sakerin, *Atmos. Oceanic Opt.* **10**, No. 8, 540–545 (1997).
6. S.M. Sakerin and D.M. Kabanov, *J. Atmos. Sci.* **59**, No. 3, Part 1, 484–500 (2002).
7. Angström, *Tellus XVI*, No. 1, 64–75 (1964).
8. V.S. Kozlov, M.V. Panchenko, A.G. Tumakov, V.P. Shmargunov, and E.P. Yausheva, *J. Aerosol Sci.* **28**, Suppl. 1, S231–S232 (1997).
9. A.D.A. Hansen, H. Rosen, and T. Novakov, *Sci. Total Environ.* **36**, No. 1, 191–196 (1984).
10. H. Rosen and T. Novakov, *Appl. Opt.* **22**, No. 1, 1265–1267 (1983).
11. A.D. Clarke, *Appl. Opt.* **21**, No. 16, 3021–3031 (1982).
12. S.M. Sakerin, D.M. Kabanov, A. Smirnov, B. Holben, I. Slutsker, and D. Giles, in: *Basic Studies of Oceans and Seas* (Nauka, Moscow, 2006) (in print).
13. S.M. Sakerin and D.M. Kabanov, *Atmos. Oceanic Opt.* **12**, No. 2, 93–98 (1999).
14. V.M. Volgin, O.A. Ershov, A.V. Smirnov, and K.S. Shifrin, *Izv. Akad. Nauk SSSR, Ser. Fiz. Atmos. Okeana* **24**, No. 10, 1058–1065 (1988).
15. Y.V. Villevalde, A.V. Smirnov, N.T. O'Neill, S.P. Smyshlyaev, and V.V. Yakovlev, *J. Geophys. Res.* **99**, 20,983–20,988 (1994).
16. M. Shiobara, J.D. Spinhirne, A. Uchiyama, and S. Asano, *J. Appl. Meteorol.* **35**, No. 1, 36–46 (1996).
17. V. Vitale, C. Tomasi, A. Lupi, A. Cacciari, and S. Marani, *Atmos. Environ.* **34**, 5095–5105 (2000).
18. V.V. Pol'kin, *Proc. SPIE* **5743**, 359–364 (2004).
19. V.S. Kozlov, M.V. Panchenko, S.A. Terpugova, V.V. Pol'kin, and E.P. Yausheva, in: *Big Vasyugan Bog. Current State and Processes of Development*, ed. by M.V. Kabanov (Publishing House of IAO SB RAS, Tomsk, 2002), pp. 156–164.
20. D.M. Kabanov and S.M. Sakerin, *Atmos. Oceanic Opt.* **13**, No. 8, 664–670 (2000).
21. S. Neshiba, *Oceanology* (Mir, Moscow, 1991), 414 pp.
22. K.K. Moorthy, S.K. Satheesh, S.S. Babu, and A. Saha, *Geophys. Res. Lett.* **32**, L14818, doi:10.1029/2005GL023267 (2005).